Internal Magnetic Field Gradients in Paramagnetic Shale Pores

M. E. Ramia & C. A. Martín

Applied Magnetic Resonance

ISSN 0937-9347

Appl Magn Reson
DOI 10.1007/s00723-017-0922-9

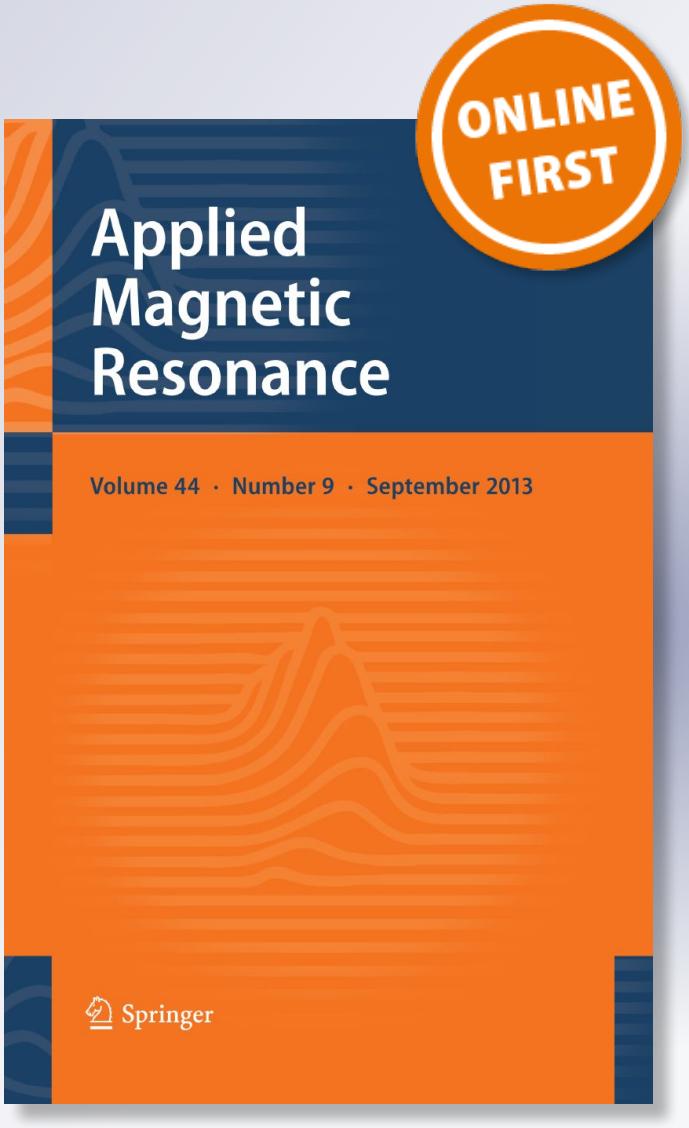

Springer

Appl Magn Reson
DOI 10.1007/s00723-017-0922-9

Applied Magnetic Resonance

REVIEW ARTICLE

Internal Magnetic Field Gradients in Paramagnetic Shale Pores

M. E. Ramia[1] · **C. A. Martín**[1]

Received: 27 March 2017 / Revised: 25 July 2017

Abstract The present work involves a comprehensive study to provide a theoretical model of the internal magnetic field gradients, present in paramagnetic shale pores, to explain the main relaxation features observed by nuclear magnetic resonance transversal relaxation measurements. In the systematic analysis process of relaxation data it is necessary to know up to what extent the magnetic field gradients are generated by the logging tool and/or arise internally in the rock due to their paramagnetic impurities content. The physical model to explain the relaxation features is based on the calculation of field gradients in a planar pore with and without relaxatives walls. The results reproduce the features of the relaxation parameters in pores due to paramagnetic and tortuous walls. The mechanism that drives the relaxation process is governed by anomalous diffusion within micro-pores. These relaxation processes arise from the interactions between the protons, belonging to the liquid molecules and the pore walls, whose structure is characterized by both large tortuosity and abundance of paramagnetic impurities, giving rise to local strong time dependent magnetic field gradients. The theoretical results are compared with those obtained experimentally to validate the relaxation model. The experimental data were gathered from a sample belonging to the "Vaca Muerta" formation of the Neuquén basin, Argentina.

1 Introduction

In natural oil porous rocks the physics of nuclear magnetic resonance (NMR) transverse relaxation is complex and a complete theoretical model describing the entire spin echo decay have not been thoroughly developed. Consequently, several

✉ M. E. Ramia
ramia@famaf.unc.edu.ar

[1] Facultad de Matemática Astronomía y Física, Universidad Nacional de Córdoba, 5000 Córdoba, Argentina

Published online: 10 August 2017

models have been proposed for spin diffusion in static magnetic fields [1]. Moreover, the complexity of the relaxation processes in shale pores yielded by both the lithology of the structure and the physicochemical composition of the pore walls are the main causes of the relaxation features. Namely, both the pore surface tortuosity and their large content of paramagnetic compounds Therefore, the standard procedures of relaxation data analysis requires of different models.

One of the most recently introduced procedures to take account of the transversal relaxation times ($T_2(t)$), although frequently used but not well grounded [2], is to describe the decay profiles by modified stretched exponential (MSE), and assuming that

$$\begin{aligned} M(t) &= M_0 \exp\left[-\frac{t}{T_2(t)}\right] \\ &= M_0 \exp\left[-\frac{t}{\tau_0}\left(1+\frac{t}{\tau_c}\right)^{\beta-1}\right] \cong \begin{cases} M_0 \exp\left[-\dfrac{t}{\tau_0}\right], & t \ll \tau_c \\ M_0 \exp\left[\left(-\dfrac{t}{\tau_D}\right)^{\beta}\right], & t \gg \tau_c \\ \tau_D = \tau_0^{1/\beta}(\tau_c)^{(\beta-1)/\beta} \end{cases} \end{aligned} \tag{1}$$

where $M(t)$ is the transversal magnetization, M_0 the initial equilibrium magnetization, β is an exponent that takes account of the degree of exponential stretching, τ_0, τ_c and τ_D are characteristic times. Being $1/\tau_0$ is the pore wall relaxation rate [1] give by the product of the NMR relaxivity, ρ, times the ratio surface to volume, (S/V), of the pore. The phenomenological interpretation of τ_c and τ_D arises from the long time limit, $t \gg \tau_c$, having the spins diffused throughout the pore volume undergoing a random process with a correlation length given by $\lambda = \sqrt{D\tau_D}$, being D the diffusion coefficient. Similarly, the value of $1/\tau_D$ represents the long time limit rate of the diffusion and wall relaxation processes.

Another assumption is to approach the total relaxation rate as driven by two mechanisms one being the volumetric term, given by

$$\frac{1}{T_{2P}} = \rho\frac{S}{V} = \frac{\rho}{a}, \tag{2}$$

where the ratio surface to volume of the pore is known as the pore size ($a = V/S$), rate that takes account of the relaxation undergone by a spin entering and leaving the wall region during a time lapse shorter than the inter-pulse time (t_e); another term affecting the relaxation being a diffusion term whose decay is described by a simple stretched exponential (SE) or Weibullian. Additionally, to circumvent the fact that as $t \to 0$ the stretched exponential rate goes to zero it is convenient to consider only the first order term of the relaxation rate [3]. This assumption is based on experimental facts whose limits are imposed by both the properties of the studied sample type and the NMR spectrometer implying that $t = 0$ is an ideal limit, being t_e the shortest time available.

2 Previous Results

Measurements of NMR transversal relaxation in shale rocks from the Vaca Muerta basin (Neuquén, Argentina) show decay profiles characterized by two simultaneous mechanisms a volumetric term and stretched exponential [3], where the total relaxation rate may be written as

$$\begin{aligned}\frac{1}{T_2(t)} &= \frac{1}{T_{2P}} + \frac{1}{T_{2D}} = \rho\left(\frac{S}{V}\right)_{\text{pore}} + \beta\left(\frac{D}{12}\gamma^2 G^2\right)^{\beta} t_{\text{e}}^{3\beta-1} \\ &= \frac{\rho}{a} + \beta\left(\frac{D}{12}\gamma^2 G^2\right)^{\beta} t_{\text{e}}^{3\beta-1},\end{aligned} \tag{3}$$

where T_{2P} and T_{2D} are the relaxation times due to interchange spin interactions with the pore wall and diffusion, respectively. In Eq. (3) S and V are the surface and pore volume, ρ the relaxivity, D the diffusion coefficient, G the z component of the magnetic field gradient (MFG), β an arbitrary exponent and t_{e} the time elapsed between magnetization refocusing radio frequency pulses (π) in a Carr-Purcell-Meiboom-Gill (CPMG) sequence [4, 5], and γ the proton gyromagnetic ratio.

The sources of such a decay behavior are the anomalous diffusion processes taking place within the pore volume subject to internal magnetic field gradients due to both magnetic impurities and tortuosity of the pore walls.

The relaxation results show clearly the existence of diffusion taking place in presence of internal magnetic field gradients, even more taking into account that the measurements were performed with the sample immersed in a homogenous external magnetic field. Figure 1 shows the T_2 relaxation data for different inter-pulse time, t_{e}, previously reported [3], which unmistakably shows the diffusion processes.

Also the NMR relaxation data show that the sample possess three pore sets, characterized by their size as small (S), medium (M) and large (L), respectively. Table 1 shows the results including the exponent (β), pore size (a), MFG (G), and pore abundance (A).

3 The Physical Model

The observed transversal relaxation decays are described by the contribution of a volumetric term and a stretched exponential. This is because the complex spreading of proton relaxation processes in the pores are subject to large internal time dependent magnetic field gradients. Some elements that contribute to this complexity are:

1. The surface of the pores is too large due to its surface tortuosity.
2. The diffusion within the pore surface is different from that in the bulk.
3. Qualitatively, the molecules residence time at the surface is greater than in the bulk (at equal effective volumes).
4. In Eq. (3) the power dependence of the relaxation at short values of both t and t_{e} is typical of molecules undergoing Levy walk diffusion [10, 11]. Where

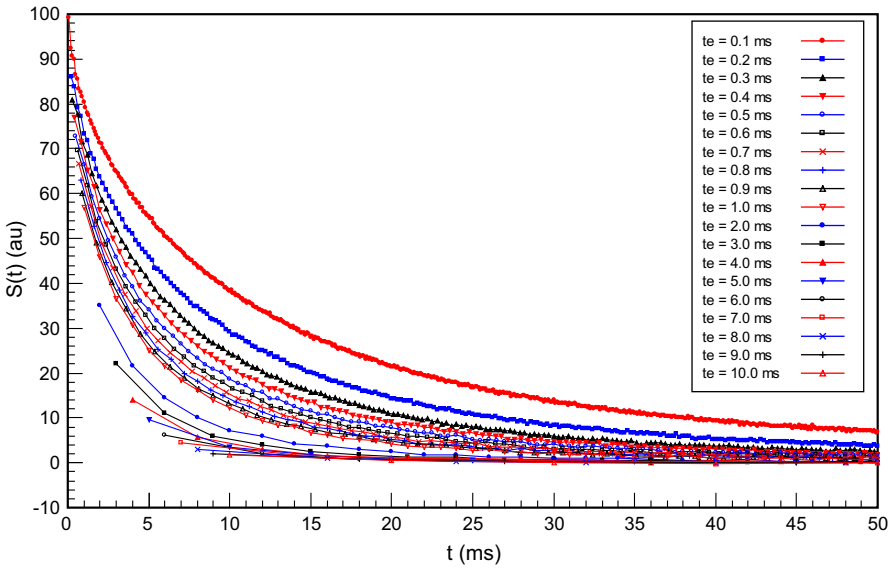

Fig. 1 T_2 decays for different t_e of the preserved sample fluids in the shale

Table 1 Experimental parameters obtain from relaxation data

i	β_i	a_i (μm)	G_i (Tm^{-1})	A_i (%)
S	0.637	2.57	31.76	17.55
M	0.561	9.51	5.561	53.85
L	0.515	20.13	1.481	28.6

$0 < \beta < 1$ is the characteristic exponent of molecules undergoing a sub diffusive dynamics, while for ordinary diffusion $\beta = 1$.

To explain the transverse relaxation phenomena, a physical model including two simultaneous mechanisms such as diffusion in the presence of internal magnetic field gradient, G, and the interchange interaction with the surface of the pore, is needed. This model should explain the main features of the experimental results because directly reflects the complexity of the pore wall region. An approximate model is to assume that the pore wall is formed by tortuous and intricate channels with flat edges where the liquid molecules diffuse, as shown in Fig. 2.

Therefore, the contribution of both pore wall tortuosity and paramagnetic impurities at the walls affects the internal MFG, G, and consequently the relaxation. Since it is impossible to provide a mathematical model of the pore wall, it is necessary to calculate G with a pore wall model to explain the experimental results and their features.

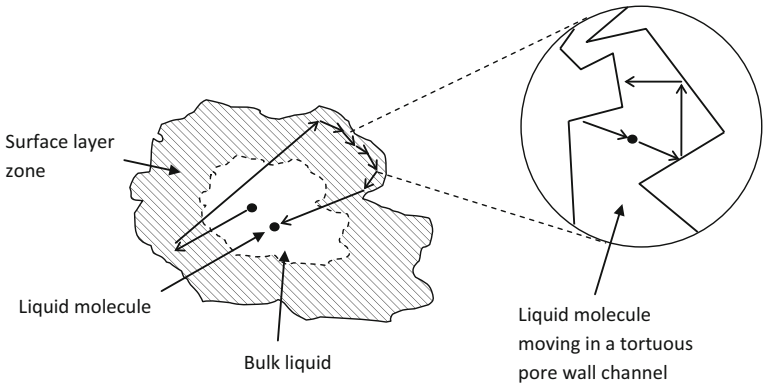

Fig. 2 Motion of a water molecule inside a pore

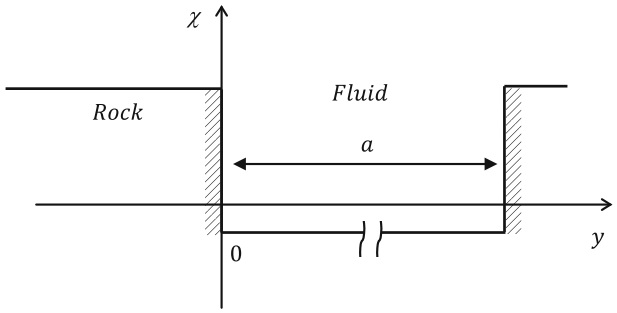

Fig. 3 Susceptibility function in a planar pore

4 The Internal Magnetic Field Gradient

The pore model used to evaluate the local MFG is a planar pore with size a, with paramagnetic impurities localized at the pore walls. This model assumes the magnetic susceptibility described by a rectangular well function spatially depending of the y coordinate, such that the discontinuity takes place at the pore walls, Fig. 3. In general the pore walls are paramagnetic while the pore fluid is slightly diamagnetic, namely

$$\chi_{\text{fluid}} = cst < 0 \quad \text{and} \quad \chi_{\text{rock}} = cst > 0. \tag{4}$$

Additionally, it is assumed that the pore walls are sufficiently far from each other so as there is no influence on each other. Whereas in the absence of radio frequency (rf) the magnetic fields are static and within a non conducting medium, to obtain the magnetic field gradient in the z direction, the general equations to be solved are

$$\begin{aligned} \boldsymbol{B} &= \mu_0(1+\chi)\boldsymbol{H} \\ \nabla \times \boldsymbol{H} &= 0 \\ \nabla^2 \boldsymbol{A} &= -\boldsymbol{B} \times \frac{\nabla \chi(r)}{(1+\chi)}, \end{aligned} \tag{5}$$

with $\boldsymbol{H} = H_0\hat{k}$ and $\boldsymbol{B} = \nabla \times \boldsymbol{A}$. Where $\boldsymbol{H}$ is the magnetic field, $\boldsymbol{B}$ the magnetic induction and $\boldsymbol{A}$ the magnetic potential vector.

Therefore, taking into account that $\chi = \chi(y)$, in this particular planar pore

$$\nabla^2\boldsymbol{A} = -\boldsymbol{B} \times \frac{\nabla\chi}{(1+\chi)} = -\mu_0 H_0 \hat{k} \times \nabla\chi = H_0 \frac{\partial\chi}{\partial y}\hat{i}. \tag{6}$$

Additionally, $\nabla \cdot \boldsymbol{A} = 0$, since the potential vector satisfies the Lorentz condition for stationary fields in non conductive media [6], condition fully satisfied in these shale pores since the fluid content is mostly oil and the shale resistivity is large compared to typical oil sand stones. Therefore, in the absence of rf from Eqs. (5) and (6)

$$-H_0 \frac{\partial\chi}{\partial y}\hat{i} = \nabla^2\boldsymbol{A} = \nabla^2 A_x\hat{i} + \nabla^2 A_y\hat{j} + \nabla^2 A_z\hat{k}, \tag{7}$$

and

$$-H_0 \frac{\partial\chi}{\partial y}\hat{i} = \nabla^2 A_x\hat{i}. \tag{8}$$

Prior to find a solution of Eq. (8), let us analyze the physical origin of the potential vector sources. From the Biot and Savart law it follows that

$$\mathrm{d}\boldsymbol{A} = \frac{\mu I}{4\pi r}\mathrm{d}\boldsymbol{l}, \tag{9}$$

where $\mathrm{d}\boldsymbol{l}$ is current I differential trajectory vector, and r the distance from the current to the point. Considering that $\boldsymbol{H} = H_0\hat{k}$, the external field that induces a polarization current segment $I\ \mathrm{d}\boldsymbol{l} = -I\ \mathrm{d}l\ \hat{i}$, thus

$$\mathrm{d}\boldsymbol{A} = -I\ \mathrm{d}l\ \hat{i}. \tag{10}$$

The classical electromagnetic model of the rock assumes that the relevant current sources of the potential vector are localized on the pore surface while those inside the rock do not contribute to the relaxation. Two particular cases are possible for sedimentary rocks, one where the paramagnetic impurities are infinitely diluted on the pore surface and the other one with a reasonable concentration such that there is a distribution of magnetization currents on the pore surface. In the first case the local field arises from point sources generates a potential vector described by Eq. (9). The second one requires to solve Eq. (8), which according to the susceptibility function (Eq. 4) results

$$\nabla^2 A_p = \mp H_0\,\Delta\chi\,\delta(y - y_a), \tag{11}$$

where $A_x(x, y, z) \equiv A_p$ is the x component of the potential vector which gives rise to the local magnetic field due to paramagnetic impurities, $\Delta\chi = \chi_{\mathrm{roca}} - \chi_{\mathrm{fluido}}$, and the $(-)$ sign corresponds to Eq. (11) valid from the fluid to the rock at the left side pore wall while the $(+)$ corresponds to the pore wall at the right side. For a single linear current singularity at every (y', z') point, with infinitely length along the x direction, the solution of Eq. (11) is

$$A_p = \frac{H_0 \Delta\chi}{4\pi} \ln\left[(y-y')^2 + (z-z')^2\right]. \tag{12}$$

The pore surface is viewed as a sheet of magnetization currents requiring integration of Eq. (12) over the source variable z' with upper and lower limits given by

$$\begin{gathered} z'_{\mathrm{l}} \ll z' \ll z'_{\mathrm{u}} \cong \sqrt{DT_1} \cong 10^{-4}\ \mathrm{m} \cong 100\ \mu\mathrm{m} \\ z'_{\mathrm{l}} = -z'_{\mathrm{u}}, \end{gathered} \tag{13}$$

where $D \cong 2 \times 10^{-9}\ \mathrm{m^2\ s^{-1}}$ is the oil measured diffusion coefficient [3], and the solution is

$$\begin{aligned} A_{\mathrm{p}} = \frac{H_0 \Delta\chi}{4\pi} \Bigg[& (z'_{\mathrm{u}} - z) \ln\left[(y-y')^2 + (z'_{\mathrm{u}} - z)^2\right] + 2|y-y'| \tan^{-1}\left(\frac{(z-z'_{\mathrm{u}})}{|y-y'|}\right) \\ & + (z - z'_{\mathrm{l}}) \ln\left[(y-y')^2 + (z'_{\mathrm{l}} - z)^2\right] - 2|y-y'| \tan^{-1}\left(\frac{(z'_{\mathrm{l}} - z)}{|y-y'|}\right) - 2(z'_{\mathrm{u}} - z'_{\mathrm{l}}). \end{aligned} \tag{14}$$

In the above equation y' takes two possible values 0 or a referred to either the left or the right pore wall, respectively. Furthermore, for simplicity, let us analyze the $y' = 0$ case. Therefore,

$$\begin{aligned} A_p = \frac{H_0 \Delta\chi}{4\pi} \Bigg[& (z'_{\mathrm{u}} - z) \ln\left[y^2 + (z'_{\mathrm{u}} - z)^2\right] + 2y \tan^{-1}\left(\frac{z'_{\mathrm{u}} - z}{y}\right) \\ & + (z - z'_{\mathrm{l}}) \ln\left[y^2 + (z'_{\mathrm{l}} - z)^2\right] - 2y \tan^{-1}\left(\frac{(z'_{\mathrm{l}} - z)}{y}\right) - 2(z'_{\mathrm{u}} - z'_{\mathrm{l}}) \Bigg] \end{aligned} \tag{15}$$

Equation from which the magnetic field due to paramagnetic impurities can be calculated, thus

$$\boldsymbol{B}_P = \nabla \times \boldsymbol{A}_p = -\hat{k}\frac{\partial A_p}{\partial y} + \hat{j}\frac{\partial A_p}{\partial z}. \tag{16}$$

Taking into account only first order secular interactions affecting the transversal relaxation, the z component of the gradient of $\boldsymbol{B}_P$ must be considered, namely

$$\nabla B_{P,z} = -\frac{\partial A_p}{\partial y} = -\frac{H_0 \Delta\chi}{2\pi}\left[\tan^{-1}\left(\frac{z'_{\mathrm{u}} - z}{y}\right) + \tan^{-1}\left(\frac{z'_{\mathrm{u}} + z}{y}\right)\right], \tag{17}$$

where it has been replaced z'_{l} by $-z'_{\mathrm{u}}$. It is important to point out that the range to consider for y in Eq. (17) is $Dt_e \le y \le a$, since any resonant nucleus at distances $0 \le y < Dt_{\mathrm{e}}$ has already relaxed after t_{e}. Since both y and z are such that $z \ll z'_{\mathrm{u}}$, and $0 < y \ll z'_{\mathrm{u}}$, Eq. (17) may be approached at lowest order by

$$\nabla B_{P,z} \approx -H_0 \Delta\chi\left(\frac{1}{2} - \frac{y}{\pi z'_{\mathrm{u}}}\right). \tag{18}$$

5 Magnetic Field Gradient

The average MFG G sensed by a spin that diffuses, during the time between rf pulses, t_e, is given by the average of $\nabla B_{P,z}$ with the free diffusion propagator $P(y_0, y, t)$ [7], being the conditional probability that a particle initially at, $t = 0$, the position y_0 reaches the position y at time t, given by

$$P(y_0, y, t) = \frac{1}{\sqrt{4\pi Dt}} \exp\left[-\frac{(y - y_0)^2}{4Dt}\right]. \tag{19}$$

Thus, the average gradient at the position y is

$$G(y) = \frac{1}{a}\int_0^a \nabla B_{p,z}(y) P(y_0, y, t) \mathrm{d}y_0. \tag{20}$$

Integrating over the initial position variable y_0, $G(y)$ becomes

$$\begin{aligned} G(y) &= -\frac{H_0 \Delta\chi}{a\sqrt{4\pi Dt}} \int_0^a \left(\frac{1}{2} - \frac{y}{\pi z'_u}\right) \exp\left[-\frac{(y - y_0)^2}{4Dt}\right] \mathrm{d}y_0 \\ &= -\frac{H_0 \Delta\chi}{a}\left(\frac{1}{4} - \frac{u}{2\pi u'}\right)\{\mathrm{erf}(\eta u) + \mathrm{erf}(\eta(1-u))\}, \end{aligned} \tag{21}$$

where the following dimensionless variable and parameter have been introduced

$$\begin{aligned} u &\equiv \frac{y}{a}, \quad 0 < u < 1 \\ 0.5 \le \eta &= \frac{a}{\sqrt{4Dt}} \le 15, \end{aligned} \tag{22}$$

therefore,

$$\begin{aligned} G(u) &= -G_0\left(\frac{1}{4} - \frac{u}{2\pi u'}\right)\{\mathrm{erf}(\eta u) + \mathrm{erf}(\eta[1-u])\} \\ G_0 &= \frac{H_0 \Delta\chi}{a}, \quad u' \equiv \frac{z'_u}{a}, \end{aligned} \tag{23}$$

the coefficient G_0 in Eq. (23) is phenomenologically assumed in the literature as the magnetic MFG inside a pore of size a generated by the static field H_0; also that the erf function possesses the following properties

$$\begin{aligned} \mathrm{erf}(-x) &= -\mathrm{erf}(x) \\ \mathrm{erf}(x) &\cong \frac{2}{\sqrt{\pi}}\left(x - \frac{x^3}{3} + \frac{x^5}{10} - \frac{x^7}{42} + \cdots\right), \end{aligned} \tag{24}$$

and taking into account the range of both η and u (Eq. 23) in Eq. (24) it is possible to expand the solution for small values of the argument, thus

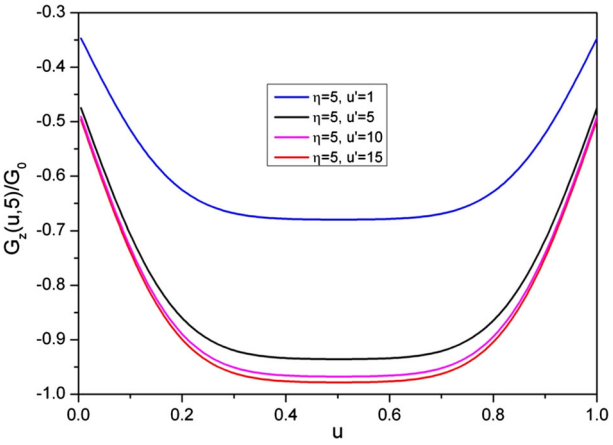

Fig. 4 MFG in a planar pore, with non relaxatives walls

$$\begin{aligned}\operatorname{erf}(\eta u)+\operatorname{erf}(\eta[1-u]) &\cong \frac{2}{\sqrt{\pi}}\left[\eta u-\frac{\eta^3u^3}{3}+\eta(1-u)-\frac{\eta^3}{3}(1-u)^3\right]\\ &\cong \frac{2\eta}{\sqrt{\pi}}\left\{1+\eta^2u(1-u)\right\},\end{aligned} \tag{25}$$

and

$$\begin{aligned}G(u) &\cong -G_0\frac{\eta}{\sqrt{\pi}}\left(\frac{1}{2}-\frac{u}{\pi u'}\right)\left\{1+\eta^2u(1-u)\right\}\\ &\approx -G_0\frac{\eta}{2\sqrt{\pi}}\left\{1+\eta^2u(1-u)\right\},\quad \text{for}\quad u'\gg u.\end{aligned} \tag{26}$$

Considering the symmetry of the pore, the contribution to G from the pore wall at a it requires to exchange

$$y\to a-y\Rightarrow u\to 1-u, \tag{27}$$

in $G(u)$ and its result added to that of Eq. (23), resulting

$$\begin{aligned}G(u) &= -G_0g(u)\{\operatorname{erf}(\eta u)+\operatorname{erf}(\eta[1-u])\}\\ G_0 &= \frac{H_0\Delta\chi}{a},\quad g_1(u)=\left(\frac{1}{2}-\frac{u}{\pi u'}\right),\quad u'\equiv\frac{z'_u}{a}.\end{aligned} \tag{28}$$

Figure 4 shows different profile corresponding to $G(u)$ with $\eta=5$ and for different possible values of $u'=1$, 5, 10, 15, respectively.

6 Diffusion Between Planes with Relaxatives Boundary Conditions

The boundary conditions imposed in a pore by relaxatives walls upon the diffusion propagator are described

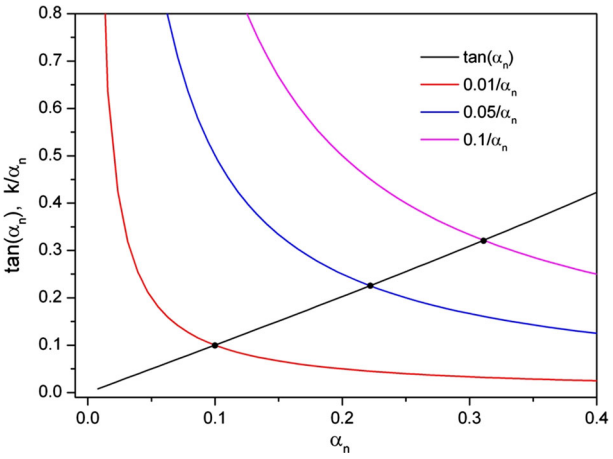

Fig. 5 tan α_n and $k\alpha_n^{-1}$ vs. α_n

$$[D\hat{\boldsymbol{n}} \cdot \nabla P + MP]_{y=0,a} = 0, \tag{29}$$

where $\hat{\boldsymbol{n}}$ is the normal direction to the surface. The solution expanded in eigenfunctions [8, 9] is given by

$$\begin{aligned} P(y_0, y, t) = \frac{1}{a}\Bigg\{ & \sum_{n=0}^{\infty}\left[1 + \frac{\sin(2\alpha_n)}{2\alpha_n}\right]^{-1} \cos\left(\frac{\alpha_n y_0}{a}\right)\cos\left(\frac{\alpha_n y}{a}\right)\exp\left(-\frac{\alpha_n^2 Dt}{a^2}\right) \\ & + \sum_{m=0}^{\infty}\left[1 - \frac{\sin(2\beta_m)}{2\beta_m}\right]^{-1} \sin\left(\frac{\beta_m y_0}{a}\right)\sin\left(\frac{\beta_m y}{a}\right) exp\left(-\frac{\beta_m^2 Dt}{a^2}\right)\Bigg\}. \end{aligned} \tag{30}$$

And the eigenvalues of the solutions α_n and β_m are the solutions of the equations

$$\begin{aligned} \alpha_n \tan\alpha_n &= \frac{Ma}{D} \equiv k \\ \beta_m \cot\beta_m &= -\frac{Ma}{D} \equiv -k. \end{aligned} \tag{31}$$

It must be remarked that the solution of Eq. (30) involves products of exponentials and harmonic functions, and those with the largest probability are the ones possessing the smallest eigen values, namely the smallest values of M. Taking into account the units of the magnitudes a and D (Eq. 31), M in units of k is

$$\begin{aligned} M &= \frac{D}{a}k \\ 5 \times 10^{-4}k \le M &\le 0.5k. \end{aligned} \tag{32}$$

Figures 5 and 6 show the graphic solutions, given at the points of intersection, of Eq. (33) and Figs. 7 and 8 the eigenvalues solutions vs. k. Figure 6 also shows the positive eigenvalues β_m, since otherwise the probability would grow indefinitely with time.

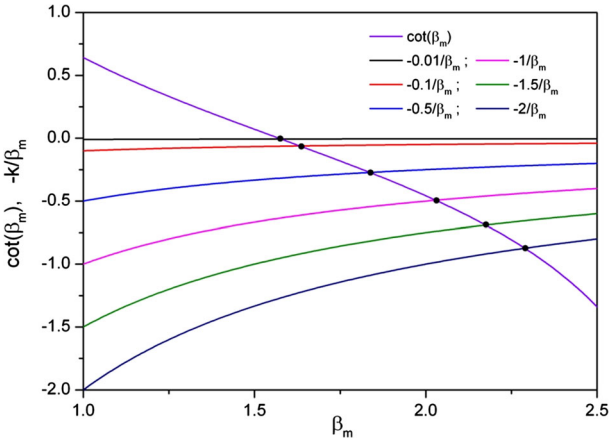

Fig. 6 $\cot\beta_m$ and $-k\beta_m^{-1}$ vs. β_m

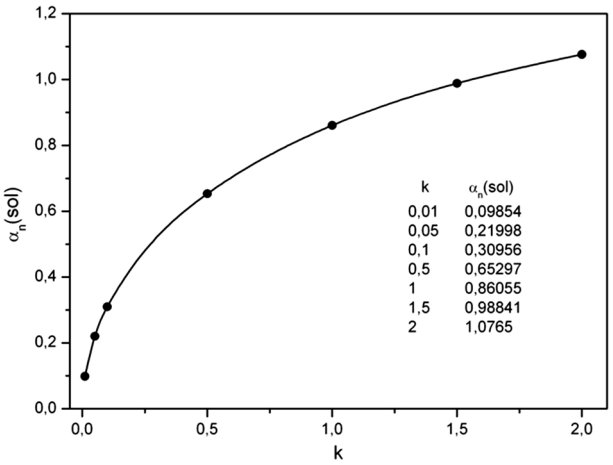

Fig. 7 α_n solution vs. k

The continuous lines in graphs represent a polynomial interpolation of the solution points. Although the interpolation does not have any physical meaning, it provides a suitable way to obtain intermediate solution points.

From the solutions it is clear that for an average values of $a \approx 10$ μm and with the time scales involved in the experiment

$$5 \times 10^{-3} \leq \frac{Dt}{a} \leq 10. \tag{33}$$

Then is reasonable an eigen value $\alpha_0 \approx 0.01$ or smaller, implying that $k \approx 0.01$, which implies that the diffusion relaxivity M, (Eq. 32), possesses at least the same order of magnitude than the measured NMR experimental relaxivity

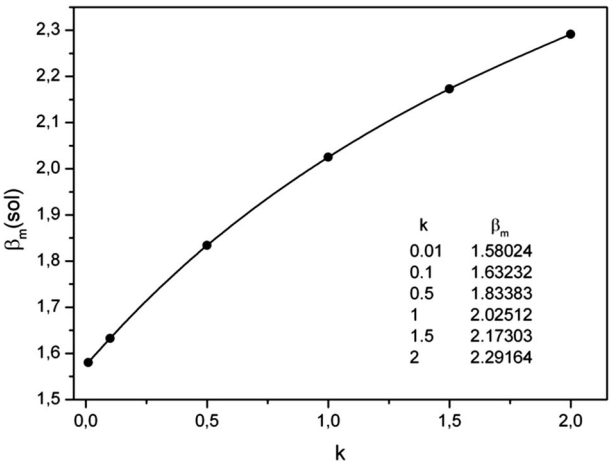

Fig. 8 β_n solution vs. k

$\rho \cong 3.3 \times 10^{-4}$ ms^{-1}. Therefore, Eq. (30) may be well approached by the addition of two zero order terms

$$P(y_0, y, t) = \frac{1}{a}\left\{\left[1 + \frac{\sin(2\alpha_0)}{2\alpha_0}\right]^{-1} \cos\left(\frac{\alpha_0 y_0}{a}\right)\cos\left(\frac{\alpha_0 y}{a}\right)\exp\left(-\frac{\alpha_0^2 Dt}{a^2}\right) + \left[1 - \frac{\sin(2\beta_0)}{2\beta_0}\right]^{-1} \sin\left(\frac{\beta_0 y_0}{a}\right)\sin\left(\frac{\beta_0 y}{a}\right)\exp\left(-\frac{\beta_0^2 Dt}{a^2}\right)\right\} \tag{34}$$

Thus, taking into account that for $k = 0.01$, $\alpha_0 = 0.09854$ and $\beta_0 = 1.58024$, Eq. (34) may be further approached by

$$P(y_0, y, t; k = 0.01) \cong \frac{1}{2a}\left[1 - \frac{\alpha_0^2}{2}\frac{(y_0^2 + y^2)}{a^2}\right]\exp\left(-\frac{\alpha_0^2 Dt}{a^2}\right) \tag{35}$$

and from Eqs. (20) and (35) yields

$$\begin{aligned} G(y) &\cong -\frac{H_0 \Delta\chi}{2a}\exp\left(-\frac{\alpha_0^2 Dt}{a^2}\right)\left(\frac{1}{2} - \frac{y}{\pi z'_u}\right)\left[1 - \frac{\alpha_0^2}{2}\left(\frac{y^2}{a^2} + \frac{1}{3}\right)\right] \\ G(u) &\cong -\frac{G_0}{2}\left(\frac{1}{2} - \frac{u}{\pi u'}\right)\left[1 - \frac{\alpha_0^2}{2}\left(u^2 + \frac{1}{3}\right)\right]\exp\left(-\frac{\alpha_0^2}{4\eta^2}\right). \end{aligned} \tag{36}$$

Even more, considering the order of magnitude of α_0^2 and the exponent in Eq. (36), then

$$G(u) \cong \frac{G_0}{2}\left(\frac{1}{2} - \frac{u}{\pi u'}\right)\left(\frac{\alpha_0^2}{2}u^2 - 1\right)\left(1 - \frac{\alpha_0^2}{4\eta^2}\right). \tag{37}$$

$$G(u) \cong \frac{G_0}{2} g_2(u)\left(1 - \frac{\alpha_0^2}{4\eta^2}\right). \tag{38}$$

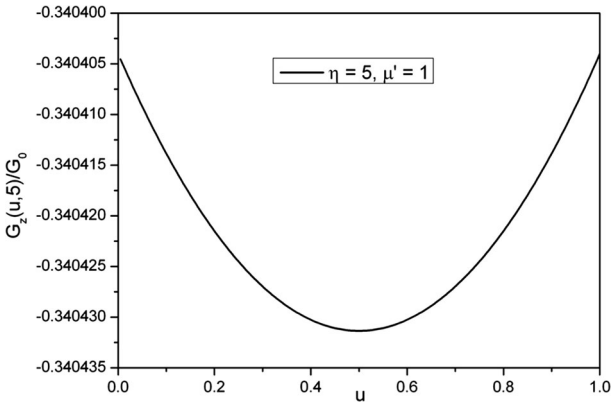

Fig. 9 MFG in a planar pore, with relaxatives walls

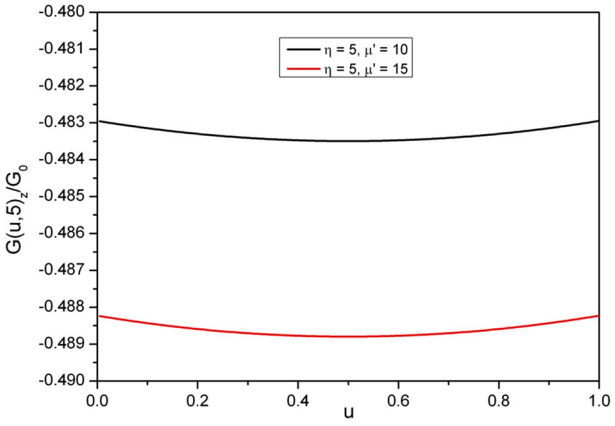

Fig. 10 MFG in a planar pore with relaxatives walls

At first glance, from both results Eqs. (28) and (37) show that the MFG described by Eq. (37) possesses maximum amplitude an order of magnitude smaller than that of Eq. (28), which is mainly dominated by the first bracket of Eq. (37). Figure 9 shows the profile corresponding to $G(u)$ with $\eta = 5$ and $u' = 1$ and Fig. 10 those for values of $u' = 10$, 15, respectively.

Notice that both results from Eqs. (28) and (37) yield through the η parameter (Eq. 20) the time dependence of the internal MFG.

Additionally, it could have been argued that restricted diffusion processes may be relevant [7], if this is so, the diffusion coefficient which was previously assumed as time independent, must be replaced by

$$D = D_0\left[1 - 0.3144\left(\frac{S}{V}\right)\sqrt{D_0 t}\right], \tag{39}$$

where D_0 is the fluid free diffusion coefficient, S the pore surface, and V its volume. Considering both the planar pore symmetry and dimensions for which their lateral planes lengths are much larger than the distance a between the pore walls

$$\frac{S}{V} \cong \frac{2}{a}, \tag{40}$$

therefore, Eq. (39) becomes

$$D \cong D_0 \left[1 - 0.6288 \frac{\sqrt{D_0 t}}{a}\right], \quad t \approx t_e, \tag{41}$$

and the parameter η becomes

$$\begin{aligned} \eta &= \frac{a}{\sqrt{4Dt}} = \frac{a}{\sqrt{4D_0 t}} \left[1 - 0.0393 \frac{\sqrt{4D_0 t}}{a}\right]^{-\frac{1}{2}} \\ &= \frac{\eta_0}{\sqrt{\eta_0 - 0.0393}}, \quad \eta_0 = \frac{a}{\sqrt{4D_0 t}}. \end{aligned} \tag{42}$$

Notice that only for the lowest values of η, (Eq. 20), Eq. (42) may be relevant, namely the second term in the bracket represents approximately the 0.8% of the whole value, while for larger values of η the approach $\eta \cong \eta_0$ is valid. Therefore, to simplify the results D may be assumed either the fluid free diffusion coefficient or the measured one to be included in the above equations.

7 Total Average MFG

The average MFG across the pore length and time is given by

$$\overline{\overline{G_z}} = \frac{1}{Ta} \int_0^T \int_0^a G_z(y) \mathrm{d}y \mathrm{d}t = \frac{1}{T} \int_0^T \int_0^1 G_z(u) \mathrm{d}u \mathrm{d}t, \tag{43}$$

where the MFG from Eqs. (28) and (36) are introduced as integrands in Eq. (43). Thus, for a pore with non relaxatives walls (Eq. 28)

$$\begin{aligned} G \equiv \overline{\overline{G_z}} &= \frac{1}{T} \int_0^T \overline{G_Z} \mathrm{d}t = -\frac{G_0}{T} \int_0^T \left[\frac{1}{2} - \frac{(e^{-\eta^2} - 1)\sqrt{\pi^{-3}}}{u' \eta}\right] \mathrm{d}t \\ \eta &= \frac{a}{\sqrt{4Dt}} = \frac{\sigma}{\sqrt{t}}, \quad \sigma = \frac{a}{2\sqrt{D}} \\ &= -\frac{G_0}{T} \int_0^T \left[\frac{1}{2} - \frac{\sqrt{\pi^{-3}}}{u' \sigma} \left(e^{-\frac{\sigma^2}{t}} - 1\right) \sqrt{t}\right] \mathrm{d}t, \end{aligned} \tag{44}$$

and

$$G = -G_0 \left\{\frac{1}{2} + \frac{\sqrt{\pi^{-3}}}{u'} \frac{2}{3} \left[2\sqrt{\pi} \eta_T^2 (\mathrm{erf}(\eta_T) - 1) - e^{-\eta_T^2} \left(\frac{1}{\eta_T} - 2\eta_T\right) + \frac{1}{\eta_T}\right]\right\}. \tag{45}$$

Taking T as the largest time during the experiment, $\eta_T \approx 0.5$ then

$$
\begin{aligned}
G &\cong -G_0\left\{\frac{1}{2}+\frac{\sqrt{\pi^{-3}}}{u'}\frac{2}{3}\left[4\eta_T^2(\eta_T-1)+2\eta_T\right]\right\}\\
&\cong -G_0\left\{\frac{1}{2}+\frac{4}{3}\frac{\sqrt{\pi^{-3}}}{u'}\eta_T[1-2\eta_T]\right\}\\
&\cong -G_0\left\{\frac{1}{2}+\frac{4}{3}\frac{\sqrt{\pi^{-3}}}{u'}\frac{a}{\sqrt{4DT}}\left[1-\frac{a}{\sqrt{4DT}}\right]\right\}.
\end{aligned}
\tag{46}
$$

Considering a pore with relaxatives walls (Eq. 36), Eq. (43) yield

$$
\begin{aligned}
G \equiv \overline{\overline{G_z}} &= -\frac{G_0}{4T}\left(1-\frac{\alpha_0^2}{2}\right)\left(1-\frac{1}{\pi u'}\right)\int_0^T \exp\left(-\frac{\alpha_0^2 Dt}{a^2}\right)\mathrm{d}t\\
&\cong \frac{G_0}{4}\frac{a^2}{\alpha_0^2 DT}\left[1-\exp\left(-\frac{\alpha_0^2 DT}{a^2}\right)\right]\\
&\approx \frac{H_0\Delta\chi}{4a}\left(1-\frac{1}{2}\frac{\alpha_0^2 DT}{a^2}+\cdots\right),
\end{aligned}
\tag{47}
$$

where $\alpha_0^2/2$ has been neglected and $u' \gg 1$ was assumed. It is important to notice that T in Eq. (47) is no longer a variable but rather a parameter the represents the time along which G has been averaged.

8 Conclusions

Notice that the results of Eqs. (28) and (38) from their dependence of the parameter η, (Eq. 20), yield both their time and pore size dependence of the internal magnetic field gradients. Also it is clear from Eq. (46) that G/G_0 is a polynomial function of a, while Eq. (47) is a polynomial in terms of a^{-1}. This feature reveals that the pore walls should be considered relaxatives. Figure 11 shows a graph of the experimental values of aG vs. a^{-1}, which is proportional to G/G_0 (the a values taken from Table 1), the red line in the plot corresponds to a fit of the data by means of a third order polynomial.

Equation (47) describes the behavior of the MFG, G, as function of both the pore size, a, and the averaging time, T. Considering the values of the different parameters involved, α_0 and D, and taking the averaging time T as the time between rf pulses, t_e, the exponent of second term in the bracket of Eq. (47) ranges approximately from 4.8×10^{-6} to 2.9×10^{-2}, therefore, for short times G behaves almost as a constant independent of t_e, while for large values it decays with t_e, as given by Eq. (47). Figure 12 shows the profiles of $G(t_e, a)$ in units of G_0 vs. t_e, for every one of the measured pore sizes, a. The t_e values are the same as those of Fig. 1.

The theoretical results show that for the smallest pore size G rapidly decrease as t_e gets longer indicating that the diffusion effects drive strong relaxation processes while for the largest pore size G decreases slower, Fig. 12. These effects explain the measured $T_2(t_e)$ previously reported [3].

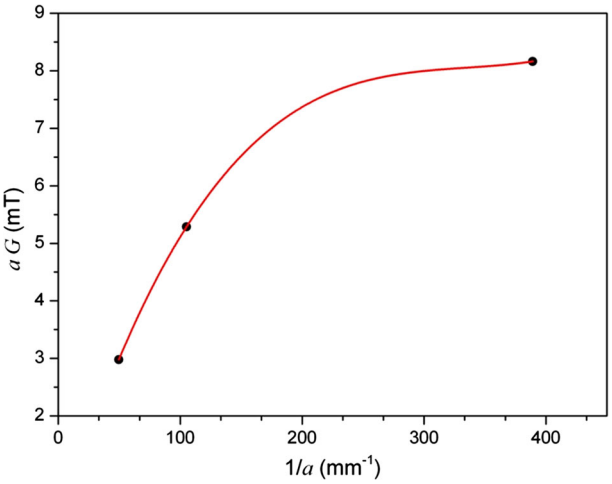

Fig. 11 Pore size times average field gradient $aG(a)$ vs. a^{-1}

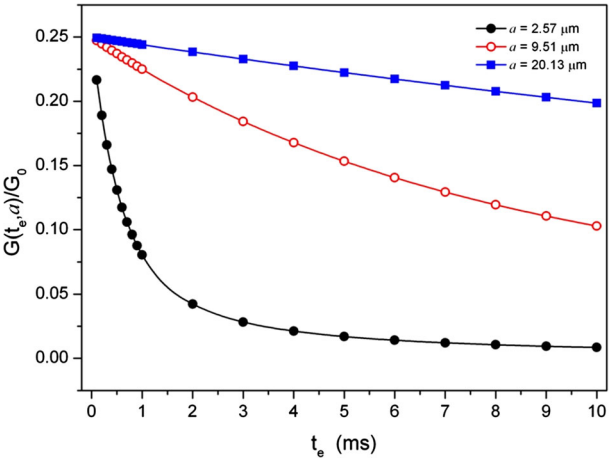

Fig. 12 MFG as a function of t_e and a vs. t_e in units of G_0

Although, the physical model is a simple approximation of the wall tortuosity and the distribution of paramagnetic impurities it is enough to explain the relaxation features. Additionally provides a base to calculate the MFG in a planar pore with and without relaxatives walls. The results explain the previously reported transversal relaxation measurements. These processes arise from the interactions between the protons, belonging to the liquid molecules, and the pore walls whose structure is characterized by both large tortuosity and abundance of paramagnetic impurities, giving rise to local strong time dependent magnetic field gradients.

Appendix: Orders of Magnitude of Variables and Constants

$$D \approx 2 \times 10^{-9}\ \mathrm{m^2 s^{-1}}$$
$$a \cong \begin{cases} 2.5 \times 10^{-6}\ \mathrm{m},\ \text{small pore sizes} \\ 25 \times 10^{-6}\ \mathrm{m},\ \text{large pore sizes} \end{cases}. \tag{48}$$

$$u \equiv \frac{y}{a}, \quad 0 < u < 1$$
$$\eta = \frac{a}{\sqrt{4Dt}}. \tag{49}$$

$$\begin{aligned} &0.1 \times 10^{-3}\ \mathrm{s} \le t \le 0.5\ \mathrm{s}\ \ \text{time range} \\ &0.1 \times 10^{-3}\ \mathrm{s} \le t_e \le 10 \times 10^{-3}\ \mathrm{s} \\ &8 \times 10^{-13}\ \mathrm{m^2} \le 4Dt \le 4 \times 10^{-9}\ \mathrm{m^2} \\ &0.04 \le \eta \le 28 \\ &1.3 \times 10^{-5}\mathrm{m} \cong \sqrt{D3T_{2L}} \le z'_u \le \sqrt{D0.5\ \mathrm{s}} \cong 3.2 \times 10^{-5}\ \mathrm{m} \\ &\quad \Rightarrow 0.1 \le u' \le 15 \end{aligned} \tag{50}$$

References

1. R.G. Coates, L. Xiao, M.G. Prammer, *NMR Logging, Principles and Applications* (Halliburton Energy Services, Houston, 1999)
2. M. Peyron, G.K. Pierens, A.J. Lucas, L.D. Hall, R.C. Stewart, J. Magn. Reson. A **118**, 214–220 (1996)
3. M.E. Ramia, C.A. Martín, Appl. Magn. Reson. **47**(10), 1323–1337 (2016)
4. C.P. Slichter, *Principles of Magnetic Resonance* (Springer, Berlin, 1990)
5. A. Abragam, *The Principles of Nuclear Magnetism* (Oxford University Press, Oxford, 1961)
6. P. Lorrain, D.R. Corson, *Electromagnetic Fields and Waves* (W.H. Freeman and Company, New York, 1970)
7. W.S. Price, *NMR Studies of Translational Motion* (Cambridge University Press, Cambridge, 2009)
8. P.T. Callaghan, *Translational Dynamics and Magnetic Resonance* (Oxford University Press, Oxford, 2011)
9. P.T. Callaghan, J. Magn. Reson. A **113**, 53–99 (1995)
10. T.F. Nonnenmacher, Phys. Lett. A **140**, 323 (1989)
11. H.F. Azurmendi, M.E. Ramia, J. Chem. Phys. **114**(2), 1 (2001)